ELSEVIER

Bioelectrochemistry 57 (2002) 39–46

Bioelectrochemistry

www.elsevier.com/locate/bioelechem

# Impedance measurements of self-assembled lipid bilayer membranes on the tip of an electrode

F. Bordi [a], C. Cametti [b,*], A. Gliozzi [c]

[a] *Dipartimento di Medicina Interna, Universita' di Roma "Tor Vergata", and INFM, Unita' di Roma I, Rome, Italy*
[b] *Dipartimento di Fisica, Università' di Roma "La Sapienza", and INFM, Unità di Roma I, Piazzale A. Moro 5 00185 Rome, Italy*
[c] *Dipartimento di Fisica, Universita' di Genova and INFM, Unita' di Genova, Italy*

Received 16 May 2001; received in revised form 16 November 2001; accepted 23 November 2001

**Abstract**

Supported lipid membranes were self-assembled on the tip of a freshly cleaved silver wire, in the presence of an appropriate polarization voltage, to facilitate, during the membrane formation, the organization of the lipids into an ordered structure. Radiowave impedance spectroscopy measurements have been carried out to provide information on the relaxation properties of the system. We have measured the conductometric and dielectric properties of bilayers built up of different lipids [dipalmitoylphosphatidic acid (DPPA), 1,2-dipalmitoyl-*sn*-glycero-3-phosphocholine (DPPC), linoleic acid (LIN)] in a wide frequency range (from $10^3$ to $10^6$ Hz) and in electrolyte solutions of different ionic strengths, in the presence of uni–univalent (KCl) and di–univalent ($CaCl_2$, $MgCl_2$, $ZnCl_2$) electrolytes. This made it possible to measure the influence of different cations and different lipid compositions on the membrane properties. In particular, we have found a different capacitive behaviour of the supported lipid bilayer membrane (s-BLM) structure in the presence of different counterions in the electrolyte solution. This peculiarity offers the opportunity for the preparation of a variety of biosensors with diverse applications in membrane biophysics, biochemistry and biotechnology. 

*Keywords:* Lipid bilayer; Supported lipid bilayer; Impedance spectroscopy; Ion transport

## 1. Introduction

Supported lipid bilayers represent a useful model system to study the basic interactions in biological cell membranes. Moreover, these systems are of great interest for technological applications, such as biosensors and molecular electronic devices [1–10].

Supported lipid bilayer membranes (s-BLMs) are currently prepared by several techniques such as monolayer transfer by Langmuir–Blodgett or Langmuir–Schaefer method, vesicle fusion, self-assembly of thiols on gold surfaces or self-assembly on the tip of a freshly cleaved silver electrode [11–15].

In the present paper, we investigate on the electrical properties deduced from frequency domain radiowave dielectric spectroscopy measurements of s-BLMs formed directly on the tip of a silver electrode [16], where during membrane formation, a negative potential was applied to achieve virtually defect-free membranes [17].

Since the membrane is assembled on an electrical conducting substrate, the system is accessible to electrical characterization by means of impedance spectroscopy from which both the structural and dynamical parameters characterizing the electrical behaviour of the membrane structure can be derived.

The application of impedance spectroscopy over a frequency range from $10^3$ to $10^6$ Hz enabled us to evaluate the membrane capacitance of the lipid bilayer and the electrical parameters (capacitance and conductance) of the ionic layer close to the lipid–electrolyte interface.

We have investigated self-assembled bilayers built up of lipids of different characteristics, i.e. zwitterionic lipids (DPPC) and ionic lipids (DPPA and linoleic acid) in the presence of electrolyte solutions of different ionic strengths, formed with uni–univalent (KCl) and di–univalent ($CaCl_2$, $MgCl_2$, $ZnCl_2$) salts. Notice that this choice allowed us to investigate the behaviour of lipids having both rigid (DPPA and DPPC) and fluid-like (linoleic acid) chains.

* Corresponding author. Fax: +39-6-4463-158.
*E-mail address:* cesare.cametti@roma1.infn.it (C. Cametti).

1567-5394/02/$ - see front matter 
PII: S1567-5394(02)00005-1

For all the systems studied, on the basis of an appropriate electrical network which represents the overall electrochemical system, we have evaluated the membrane capacitance of the supported lipid bilayers, whose values markedly depend on the counterions present in the electrolyte solution, bathing the lipid membranes. This peculiar feature allows one to consider them a useful starting point for the construction of biosensors.

## 2. Materials and methods

### 2.1. Materials

The phospholipids 1,2-dipalmitoyl-*sn*-glycero-3-phosphocholine (DPPC) and dipalmitoylphosphatidic acid (DPPA) were purchased from Sigma (St. Louis, MO). Linoleic acid (*cis*, *cis*, -9, 12-octadecadienoic acid) (LIN) was obtained from Fluka (Milan, Italy). Decane and all inorganic salts (p.a. grade) were from Merck (Darmstadt, Germany). All chemicals were used without further purification. Solutions at the desired salt concentration were prepared with Q-quality water (Millipore, Bedford, USA), with an electrical conductivity at room temperature of about $2 \times 10^{-6}$ S/m. The lipid membranes were formed on the tip of freshly cut Teflon-coated silver wire. We employed silver wire (diameter 0.37 mm), purchased from World Precision Instruments (Sarasota, USA).

### 2.2. Membrane formation

Supported self-assembled lipid membranes were obtained following the procedure described by Tien and Salamon [16]. The tip of the Teflon-coated silver wire was immersed in a phospholipid, dissolved at a concentration of 10 mg/ml, in an organic solvent (decane) or directly in the pure liquid lipid (linoleic acid). While immersed in the lipid solution, the tip of the wire is cut off with a sharp blade. The freshly cut metallic surface has a great affinity for lipid molecules which adhere to the surface itself with a variety of possible structures, the most common of which consists of two layers facing one another with the polar (hydrophilic) heads of the lipid molecules exposed to the aqueous phase. The new wire tip, coated with the lipid solution forming a self-assembled lipid layer, was subsequently transferred into the appropriate saline solution. In order to ensure a successful membrane formation, it is important to provide a freshly cut metal surface so that the whole surface electrode at the interface with the bathing solution is in the reduced state. To this end, a dc polarization electrical potential of $-450$ mV ($-350$ mV in the case of linoleic acid) is applied between the silver electrode and the ground electrode. Within a few minutes, a self-assembled, stable lipid structure adsorbed on the metallic substrate is formed. The negative potential applied during the membrane formation prevents the oxidation of the silver tip and favours the formation of defect-free membranes [17]. Membrane formation was monitored by measuring the overall electrical impedance between the electrodes (see Fig. 1), and the bilayer is considered as completely formed when the electrical parameters of the membrane have reached a steady-state value. An s-BLM formed in this manner is remarkably stable.

### 2.3. Impedance measurements

The dielectric and conductometric spectra of supported membranes have been measured in the frequency range from 1 kHz to 1 MHz, by means of a radio frequency Impedance Analyzer, Hewlett-Packard (Japan) model 4192A. The Impedance Analyzer is controlled by means of a personal computer and a complete spectrum in the whole frequency range studied, 60 frequency points logarithmically spaced, can be collected in a few seconds. The amplitude of the alternate voltage applied to the electrodes had a value of 100 mV, and, as stated above, a dc bias

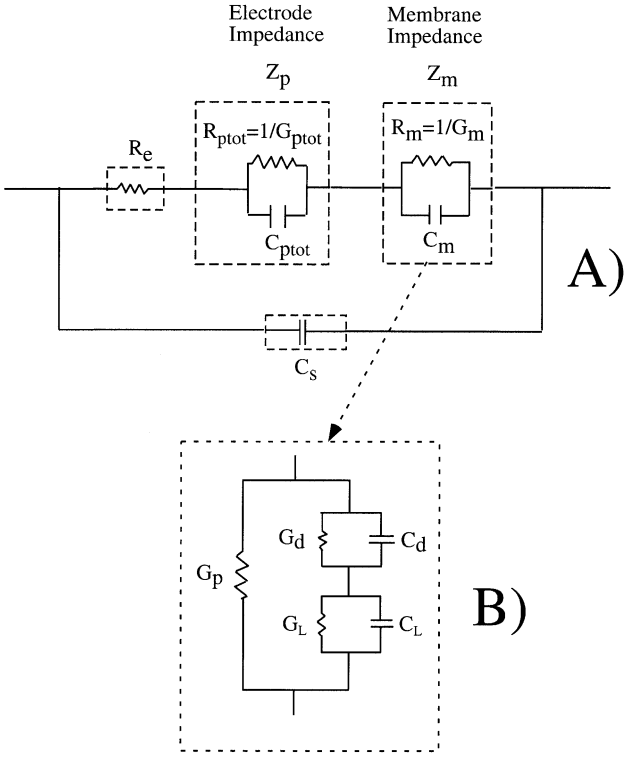


Fig. 1. (A) A simple equivalent circuit of the metal-supported lipid bilayer. The simplicity of this circuit reduces possible misinterpretations of the measured data. $C_m$ and $G_m$ represent the membrane capacitance and conductance at the interface between the electrolyte solution and the metal electrode, $C_p$ and $G_p$ are the capacitance and conductance of the electrode–electrolyte interface, $R_e$ is bulk electrolyte resistance and $C_s$ is the stray capacitance of the measuring cell. (B) The equivalent circuit of the supported lipid bilayer at the tip of the metal electrode. $C_L$ and $G_L$ represent the capacitance and conductance per unit surface of the lipid film at the electrode interface, $C_d$ and $G_d$ are the corresponding quantities at the lipid–electrolyte interface and $G_p$ is the conductance of the water pore of the uncovered region of the electrode surface.

voltage of −450 mV (or −350 mV) has been superimposed to the alternate potential.

A two-electrode setup was used, with the Teflon-covered Ag wire which supports the membrane as the working electrode and an Ag/AgCl electrode as the reference electrode. In some measurements, a non-chlorided silver wire was used as the reference electrode. In the frequency range investigated, the use of a non-reversible electrode does not induce any appreciable difference in the measured values of the dielectric parameters of the supported membranes.

To minimize the capacitive parasitic effects that, in principle, could affect the electric measurements, the two electrodes were placed on hold into the glass cell filled with the electrolyte solution by means of a silicon rubber spacer, the glass cell was surrounded by a metallic shield connected with the instrument ground and short cables were used to connect the cell to the instrument.

All measurements were carried out at room temperature (25 °C).

### 2.4. The equivalent circuit

A simple equivalent circuit was chosen to describe the most important electrical features of the electrochemical system studied (Fig. 1). Due to the intrinsic complexity of the system and the consequent poor reproducibility observed in dielectric measurements, we have analyzed the dielectric and conductometric data by employing a substitution method that allows to extract the dielectric parameters of the membrane from the measured impedance spectra. This choice can be objected owing to its roughness, but we have preferred the simplest, and hence, the more "robust" calibration procedure, to avoid misinterpretation in experimental data, as far as possible. Moreover, the simplicity of this circuit reduces possible misinterpretation of the measured data.

In the electrical network which models the electrochemical system (Fig. 1), the membrane impedance $Z_m$ is represented by a capacitance $C_m$ and a resistance $R_m$ in parallel. In series with the membrane impedance, there is the resistance of the bulk electrolyte and of the connecting cables, $R_e$, and, moreover, the impedance $Z_p$ of the reference electrode. A capacitance $C_s$ in parallel stands for the overall stray capacitance toward the ground.

The equivalent circuit is shown in Fig. 1. The membrane impedance is obtained, in the limit $C_s \ll C_{tot}$, from the total measured impedance $Z_{tot}$

$$Z_{tot} = \frac{1}{G_{tot} + i\omega C_{tot}} \tag{1}$$

by subtracting the contribution of the electrode polarization impedance and the resistance $R_e$, according to

$$\frac{1}{G_m + i\omega C_m} = \frac{1}{G_{tot} + i\omega C_{tot}} - R_e - Z_p \tag{2}$$

The membrane capacitance $C_m$ and the membrane conductance $G_m$ are given by

$$C_m = -\frac{\Im[\Delta Z]}{\omega\{(\Re[\Delta Z])^2 + (\Im[\Delta Z])^2\}} \tag{3}$$

and

$$G_m = \frac{\Re[\Delta Z]}{(\Re[\Delta Z])^2 + (\Im[\Delta Z])^2} \tag{4}$$

where $\Re[\Delta Z]$ and $\Im[\Delta Z]$ are the real and imaginary parts of the quantity

$$\Delta Z = \frac{G_{tot} - i\omega C_{tot}}{(G_{tot})^2 + (\omega C_{tot})^2} - R_e - Z_p \tag{5}$$

and $\omega$ is the angular frequency of the applied electric field.

This procedure is of course based on the assumption that the reference electrode impedance does not change with the changes in the current and that impedance at the metal–membrane interface or at the metal–electrolyte (in the absence of the membrane) remains the same. However, since these assumptions are not exactly fulfilled and a difference in the two interfaces might result, the equivalent circuit of the membrane structure (see Fig. 1B) takes into account the presence of a residual interface polarization through the capacitance $C_d$ and the conductance $G_d$ in series with the membrane itself.

A typical spectrum in the frequency range from 1 kHz to 1 MHz of the membrane capacitance $C_m$ and membrane conductance $G_m$ is given in Fig. 2. These quantities reflect the frequency behaviour of the permittivity $\varepsilon'$ (the capacitance $C_m$) and of the conductivity $\sigma$ (the conductance $G_m$), respectively, of the membrane.

The spectrum is characterized by a dielectric dispersion centered at about $10^4$ Hz, even if the low-frequency tail is not completely resolved and the low-frequency limit values fall outside the frequency window investigated. This difficulty can be partially overcome by fitting simultaneously

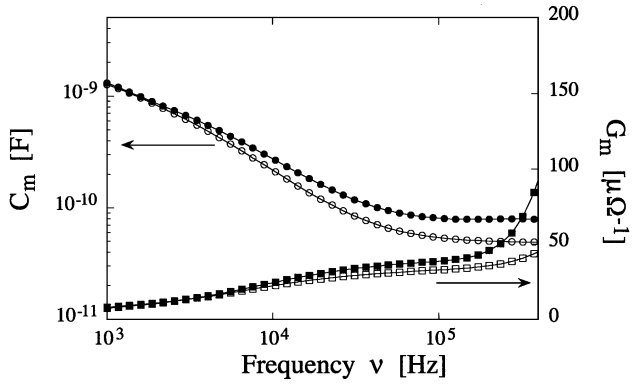


Fig. 2. The capacitance $C_m$ and the conductance $G_m$ of the lipid bilayer at the interfacial region between the electrode and the bulk aqueous phase, as a function of frequency in the range from 1 kHz to 1 MHz, for two different values of the ionic concentrations: (open symbols): DPPC/decane in 1 mM KCl; (full symbols): DPPC/decane in 10 mM KCl.

the real part (the conductance $G_m$ or, equivalently, the conductivity $\sigma$), and the imaginary part (the capacitance $C_m$, or equivalently the permittivity $\varepsilon'$) of the complex admittance to a Cole–Cole dielectric relaxation function

$$\frac{1}{i\omega\varepsilon_0}Y_m(\omega) = C_m(\omega) + \frac{G_m}{i\omega\varepsilon_0} = \frac{\Delta C_m}{1+(i\omega\tau)^{\alpha}} + C_\infty + \frac{G_0}{i\omega\varepsilon_0} \quad (6)$$

This procedure yields the dispersion parameters $\Delta C_m = C_m|_{\omega=0} - C_\infty$, the low-frequency conductance $G_0$, the relaxation time $\tau$ and the parameter $\alpha$ taking into account the spread of the relaxation time. In the above procedure, in order to reduce the number of free parameters, we have fixed the parameter $\alpha$ to the value $\alpha = 0.8$. The overall accuracy of the above procedure is reasonably good and we are able to describe the frequency behaviour of $C_m$ and $G_m$ over the whole frequency range from 1 kHz to 1 MHz.

We have investigated the dielectric behaviour of membranes formed with different ionic and zwitterionic lipids (linoleic acid, DPPA, DPPC) dissolved in an organic solvent (decane), in the presence of monovalent ($K^+$) and different divalent cations ($Ca^{++}$, $Mg^{++}$, $Zn^{++}$), at an appropriate ionic strength. In all the electrolyte solutions employed, the anion was $Cl^-$.

In order to have approximately the same electrode polarization effects in the presence of the different cations, the ionic conductivity of the bulk electrolyte solutions is approximately the same for all the systems investigated. In the following, we will summarize the main results obtained in the different solid-supported lipid bilayers used.

### 2.5. Formation and stability of the membrane

The membrane formation is monitored by following the time variation of the impedance $Z_m$. In most cases, a steady-state value is reached within about 30 min. A typical behaviour is shown in Fig. 3 for DPPC in KCl 1 mM where the constant value of the measured electrical impedance indicates a stable membrane structure (maintained for time interval of several hours).

For all the lipids studied, we have observed, within a few trials, the formation of a stable membrane, even if the number of the attempts needed to obtain the formation of a membrane increases according to the following order: linoleic acid < DPPC < DPPA. The initial change of both $C_m$ and $G_m$ can be due, at least partially, to a re-organization of the membrane at the tip of the electrode. It is noteworthy that the applied polarization voltage seems to favour the membrane formation and its stability. In fact, after membrane formation, if the polarization voltage is suddenly switched off, the membrane capacitance decreases at first, and then increases well above the original plateau value (data not shown). This behaviour suggests that switching off

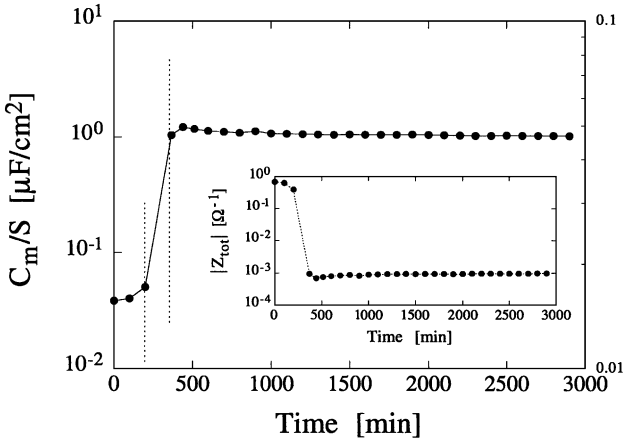


Fig. 3. The time evolution of the capacitance $C_m$ normalized to the electrode surface during the process of the membrane formation. The lipid employed is DPPC in 10 mM KCl electrolyte solution. The inset shows the time evolution of the measured total impedance (at the frequency of 5 kHz) in the same experimental conditions.

the polarization potential destabilizes the membrane structure and, due to the increased disorder, a rapid intake of water into the bilayer follows. This enhances the bilayer polarizability, causing an increase of the observed membrane capacitance.

As a test of mechanical stability, membranes formed in different conditions (after a convenient time interval from the formation, to ensure the membrane stabilization) were repeatedly extracted from the electrolyte solution and immediately re-immersed afterwards. After each step, the measured capacitance showed an abrupt change, in most cases, an increase by a factor of 2 or more, but in some cases even a decrease, indicating that, due to the extraction and re-immersion procedure, the membrane structure could be damaged in an unpredictable way. However, the electrical behaviour of the overall lipid structure remains qualitatively the same. Finally, we have investigated the membrane stability over very long time interval, of the order of a day. The results from these measurements are consistent with a slow degradation of the membrane, probably caused by a gradual opening of aqueous pores.

## 3. Results

It is well known [2] that resistivities for deposited membranes are generally smaller than those for unsupported BLMs. For all the molecular assemblies obtained at the electrode–electrolyte interface, a membrane resistivity of the order of $10^3$ Ω cm$^2$ was measured. Since unsupported BLMs exhibit very high resistivities, of the order of $10^7$–$10^8$ Ω cm$^2$, in the present experimental conditions, when a supported membrane is created, the main contribution to the membrane resistance originates from the resistance in defect pores spanding across the molecular aggregates. As pointed out by several authors [10,18], the coverage of a surface by

a layer of lipid molecules is an extremely difficult task since the morphology of the substrate at a molecular level is unlikely to be smooth and consequently, a large number of defects in the resulting monolayer or multilayers originates.

In order to determine the electrical parameters (the membrane capacitance and the capacitance and conductance of the ionic layer at the lipid–aqueous interface) associated with the lipid bilayer, the structure of the metal–lipid–aqueous phase interface must be modelled by an appropriate electrical circuit [5]. Since the lipid bilayer does not completely cover the tip of the electrode and bilayer parts, and uncovered regions coexist at the metal interface, we assume that the electrical behaviour of the whole metal–electrolyte system can be described by the equivalent circuit depicted in Fig. 1B, where $G_L$ and $C_L$ represent the conductance and capacitance per unit surface of the lipid coverage layer, $G_d$ and $C_d$, the corresponding quantities of the ionic layer connected in series at the lipid–electrolyte interface, and $G_p$, the conductance per unit surface of the uncovered region of the electrode. It should be noted, however, that according to the substitution procedure we have adopted in order to correct for the bulk electrode polarization effect, $G_d$ and $C_d$ represent the electrical parameters associated to the local different structures of the ion distribution at the lipid–electrolyte interface between covered and uncovered electrodes, rather than the conductance and capacitance of the ionic diffuse double layer at the electrode–electrolyte interface. With this picture, the measured conductance, $G_m$, and the measured capacitance, $C_m$, as a function of the angular frequency, $\omega$, in the limit $G_L \ll G_d$, $G_p$, are given by

$$G_m = (1-s)G_p + sG_d\left(\frac{\omega^2 C_L^2/G_d^2}{1+\omega^2(C_L+C_d)^2/G_d^2}\right) \quad (7)$$

and

$$C_m = sC_L\left(\frac{1+\omega^2 C_d(C_L+C_d)/G_d^2}{1+\omega^2(C_L+C_d)^2/G_d^2}\right) \quad (8)$$

where $s$ is the relative area fraction of the covered electrode and the quantity $\tau$, defined by

$$\tau = \frac{C_L+C_d}{G_d} \quad (9)$$

can be interpreted as an "apparent" relaxation time of the dispersion observed in the frequency range investigated. Although both the above expressions Eqs. (7) and (8) do not exactly follow a single Debye-type relaxation function (or, more generally, a Cole–Cole relaxation function), nevertheless, for values of the parameters of the order of those employed here, their deviations are relatively small. This justifies the analysis of the measured admittance $Y_m = G_m + i\omega C_m$ performed on the basis of Cole–Cole relaxation function. Fig. 4 shows the dependence of $C_m$ and $G_m$ (Eqs. (7) and (8)) on the frequency $\omega$ compared with that expected for a Debye-type behaviour (solid lines in Fig. 4). As can be seen, for $C_L/(C_L+C_d) \to 1$ and $C_d/(C_L+C_d) \to 0$, the frequency dependence can be approximated by a simple Debye-type relaxation. It must be noted that, owing to the equivalent electrical circuit (Fig. 1B), we would expect two different charging processes, one of which, the charging of the double layer residual capacitance, $C_d$, and the other, the charging of the membrane capacitance, $C_L$. However, due to the very high membrane resistance, these processes occur at significantly different time constants and consequently only the membrane charging dominates in the frequency part of the impedance spectrum investigated.

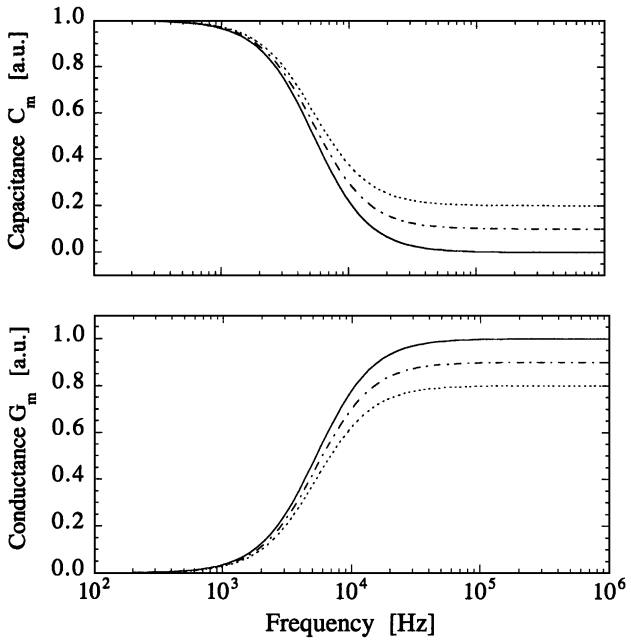


Fig. 4. Deviation of the capacitance $C_m$ (Eq. (8)) and the conductance $G_m$ (Eq. (7)) from a single Debye-type relaxation function for different values of the equivalent electrical circuit parameters. Capacitance $C_m$: full line, Debye-type behaviour, $C_d/(C_L+C_d)=0$; (–...–...–): $C_d/(C_L+C_d)=0.1$; (... ... ...) $C_d/(C_L+C_d)=0.2$. Conductance $G_m$: full line, Debye-type behaviour, $C_L/(C_L+C_d)=1$; (–...–...–): $C_L/(C_L+C_d)=0.9$; (... ... ...) $C_L/(C_L+C_d)=0.8$.

In the analysis that follows, because of the very high value (of the order of $10^7$–$10^8$ Ω cm$^2$ of a defect-free lipid membrane), the membrane resistance was not exactly detectable and therefore, as we have stated above, we assumed $G_L \ll G_p$, $G_d$. Under these assumptions, we have analyzed the measured capacitance and conductance on the basis of Eqs. (7) and (8), and the values of electrical parameters $C_L$, $G_d$, $G_p$ and the relaxation time $\tau$ have been estimated. These parameters were determined by a simultaneous non-linear least-squares fit of Eqs. (7) and (8) to the measured values. The minimization procedure, based on five adjustable parameters, allows the capacitance $C_L$ to be determined within an uncertainty of about 2–5%, with a confidence level of 0.95, whereas the estimation of the other parameters is less accurate, reflecting in a larger uncertainty (of the order of 20%). A typical behaviour of DPPC/decane in $ZnCl_2$ 0.6 mM electrolyte solution is shown in Fig. 5. As

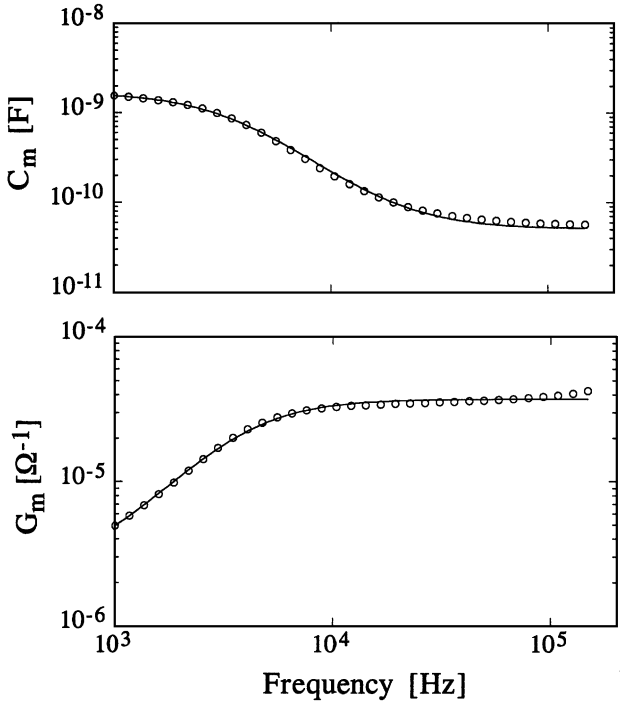


Fig. 5. A typical frequency dependence of the membrane capacitance $C_m$ and the membrane conductance $G_m$ for DPPC in 10 mM KCl electrolyte solution. The solid line represents the calculated values according to Eqs. (7) and (8). The values of the parameters deduced from the fitting procedure are listed in Table 1.

can be seen, a satisfactory agreement is obtained between measured and calculated values over the entire frequency range investigated.

The model depicted in Fig. 1B furnishes the value of the membrane capacitance, $C_L$, and those of the electrical parameters of the ionic double layers, at the electrolyte solution interface and moreover the fraction $s$ of the membrane coverage. As shown in Table 1, the values of the electrical parameters are markedly different for DPPA and DPPC in decane, for all the different electrolyte species investigated. For example, in the former case, we observe a coverage fraction of about 0.40, whereas, in the second case, values close to unity have been obtained. Analogously, by changing from DPPA to DPPC, the values of $C_d$ vary over an order of magnitude. The reliability of the above quoted figures can be partially questionable owing to the large uncertainties that affect this quantity in consequence of the partial correlation between the different parameters entering in Eqs. (7) and (8). Nevertheless, the marked difference in the two different experimental conditions point out a qualitatively different behaviour of the two phospholipids. The strong electrostatic interactions and chain stiffness, in the case of DPPA, makes it more difficult to use in the formation of an ordered structure. Accordingly, a larger number of trials were needed to obtain the electrode coverage.

Now we will discuss in detail the meaning of the different parameters obtained. Table 1 summarizes the values of $C_L$ obtained for all the systems investigated. Although the experimental technique is rather rough and the model employed to analyze the data rather crude, the technique is able to evidence a different capacitive behaviour in the three systems investigated, resulting in different membrane capacitances and indicating the different structural arrangements of the lipid bilayer. The membrane capacitance decreases in the order from about 2 μF/cm$^2$ for linoleic acid, to about 1.5 μF/cm$^2$ for DPPC and to 0.5–0.6 μF/cm$^2$ for DPPA. The absolute values of the capacitance for linoleic acid and DPPC are higher than those expected for a typical lipid bilayer. Several factors might be responsible for such behaviour. An increased value of the membrane permittivity due to water penetration inside the outer portion of the chains, the presence of a simple monolayer or a highly disordered configuration of the lipids could decrease the effective thickness of the membrane and thus produce an increase in the electrical capacitance. Moreover, due to the alkane solubility, lipid arrangements in the presence of decane could contain an amount of decane that might contribute to reduce the lipid film thickness. Specific capacitances higher than those generally expected for BLM imply a disorder and a loose packing of the phospholipids in the first transferred monolayer, causing a not-well-organized struc-

Table 1
Values of the electrical parameters of self-assembled lipid bilayer membranes on the tip of a silver electrode

| Lipids | Organic solvent | Bulk electrolyte composition | Electrical conductivity of bulk electrolyte (S/m) | Debye length (nm) | $C_L$/S (μF/cm$^2$) | Lipid film thickness (nm) | $\tau$ ($s$) | $s$ | $G_p$/S (S/cm$^2$) | $C_d$/S (μF/cm$^2$) | $G_d$/S (S/cm$^2$) |
|---|---|---|---|---|---|---|---|---|---|---|---|
| Linoleic acid | – | KCl, 10 mM | $1.43 \times 10^{-1}$ | 3.1 | $2.1 \pm 0.1$ | 1.1 | $6.1 \times 10^{-5}$ | 0.99 | 55 | 0.46 | $4.2 \times 10^{-2}$ |
| DPPA | decane | KCl, 1 mM | $1.47 \times 10^{-2}$ | 9.7 | $0.88 \pm 0.03$ | 2.5 | $1.8 \times 10^{-5}$ | 0.40 | $2.8 \times 10^{-3}$ | 0.92 | 0.10 |
| | | $CaCl_2$, 0.6 mM | $1.47 \times 10^{-2}$ | 7.4 | $0.42 \pm 0.02$ | 5.3 | $8.9 \times 10^{-6}$ | 0.40 | $3.4 \times 10^{-3}$ | 0.38 | 0.09 |
| | | $MgCl_2$, 0.6 mM | $1.47 \times 10^{-2}$ | 7.4 | $0.65 \pm 0.04$ | 3.4 | $1.0 \times 10^{-5}$ | 0.35 | $1.6 \times 10^{-3}$ | 0.35 | 0.10 |
| | | $ZnCl_2$, 0.6 mM | $1.54 \times 10^{-2}$ | 6.8 | $0.72 \pm 0.03$ | 3.1 | $1.1 \times 10^{-5}$ | 0.40 | $2.3 \times 10^{-3}$ | 0.17 | 0.08 |
| DPPC | decane | KCl, 1 mM | $1.47 \times 10^{-2}$ | 9.7 | $1.48 \pm 0.04$ | 1.5 | $4.2 \times 10^{-5}$ | 0.99 | 19 | 0.09 | $3.7 \times 10^{-2}$ |
| | | $CaCl_2$, 0.6 mM | $1.47 \times 10^{-2}$ | 7.4 | $1.07 \pm 0.03$ | 2.1 | $4.3 \times 10^{-5}$ | 0.99 | 55 | 0.05 | $2.6 \times 10^{-2}$ |
| | | $MgCl_2$, 0.6 mM | $1.47 \times 10^{-2}$ | 7.4 | $1.57 \pm 0.04$ | 1.4 | $8.2 \times 10^{-5}$ | 0.99 | 15 | 0.06 | $2.0 \times 10^{-2}$ |
| | | $ZnCl_2$, 0.6 mM | $1.54 \times 10^{-2}$ | 6.8 | $1.60 \pm 0.06$ | 1.4 | $4.8 \times 10^{-5}$ | 0.99 | 21 | 0.05 | $3.4 \times 10^{-2}$ |

Average and standard deviation of the data are collected on three or four different preparations for each sample.

ture according to the ideal structure of a Langmuir–Blodgett bilayer.

In particular, the value of $C_L$ observed for the linoleic acid ($C_L = 2$ μF/cm$^2$), assuming a dielectric constant of the hydrophobic tail region of about $\varepsilon = 2.5$, yields a lipid film thickness of about 1 nm. In the case of DPPC, the capacitances per unit surface (in the presence of KCl, $MgCl_2$ and $ZnCl_2$) are of the order of $C_L = 1.5$ μF/cm$^2$, suggesting a lipid film of apparent thickness of about 1.5–2 nm and, finally, for DPPA, to values of $C_L$ in the range 0.7–0.9 μF/cm$^2$, correspond to an apparent film thickness of between 2.5 and 5 nm, respectively. Although the thickness of the lipid film, deduced from capacitance measurements, are too thin to be that of well-organized lipid arrangement, nevertheless, the different values observed should suggest a possible different lipid organization that could be a monolayer membrane hydrophobically adsorbed on the electrode in the case of linoleic acid, a mixed monolayer–bilayer structure in the case of DPPC and finally a mixed structure, some parts of which covered by a bilayer, and some parts by a trilayer arrangement, in the case of DPPA.

This picture is in agreement with that as suggested by Passechnik et al. [5], on the basis of specific capacitance, electrostriction and surface potential measurements on s-BLMs. Moreover, the formation of monolayer, bilayer and trilayer membranes on a silver pad on the basis of ellipsometric measurements has been recently suggested by Chiang et al. [19]. A sketch of the possible lipid structures at the electrode interface is depicted in Fig. 6, together with the equivalent circuit employed in the analysis of the data. A further confirmation to the proposed structure has been recently given by Haas et al. [17]. In fact, it was shown that in the case of linoleic acid, application of a negative potential during membrane formation leads to the disappearance of oxidation–reduction peaks and therefore to a virtually "defect-free" membrane. This indicates that oxidized silver leads to defect formation. Actually, this surface should be much more hydrophilic than pure metal. Therefore, application of a negative potential should favour a hydrophobically adsorbed monolayer. However, almost complete coverage can be obtained only with DPPC and linoleic acid. This indicates that in the case of negatively charged lipids, complete coverage can be obtained only when the chains are in the fluid state.

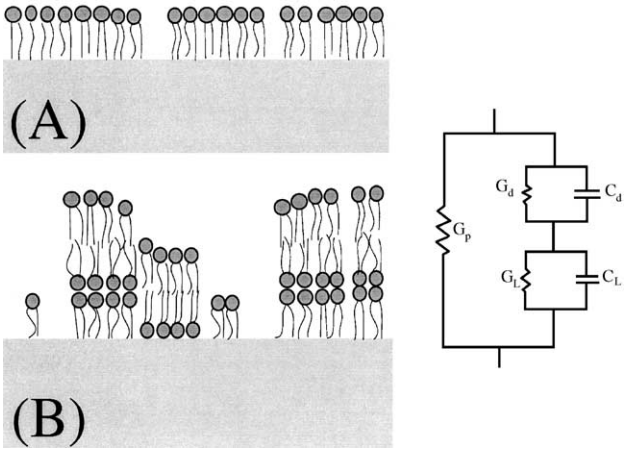


Fig. 6. A sketch of the possible arrangements of the lipid film at the electrode surface. (A) A monolayer structure (linoleic acid with a high coverage, $s = 0.99$). (B) A complex structure formed by monolayers, bilayers and trilayers (DPPA with a low coverage ($s = 0.40$) or DPPC with a high coverage ($s = 0.99$)).

The main observation derived from these findings is the high sensitivity of the charged membranes to different species of ions in solution. In fact, with zwitterionic lipids (DPPC), the values of $C_L$ are roughly around 1.5 μF/cm$^2$ for all the cations studied (with the exception of $Ca^{++}$), whereas with ionic lipids (linoleic acid and DPPA), $C_L$ varies from about 0.9 μF/cm$^2$ for monovalent cations to values between 0.4 and 0.7 μF/cm$^2$ for divalent cations (in the order, $Ca^{++}$, $Mg^{++}$ and $Zn^{++}$). Moreover, it should be noted that in the case of $CaCl_2$ electrolyte solutions, a considerable lower value of the surface capacitance for both the DPPC and DPPA systems was observed. This implies a larger lipid film thickness, probably caused by the presence of $Ca^{++}$ ions, which favour a multilayer arrangement.

As far as the other parameters are concerned, the value of $G_p$ is directly related to the metal–electrolyte interface of the uncovered electrode region and hence to the bulk ionic conductivity of the aqueous phase, bathing the electrode. Assuming a thickness of the ionic layer of the order of the Debye length and an electrode surface of $1 \times 10^{-3}$ cm$^2$, we expected values of $G_p$ of the order of 10–100 Ω cm$^2$. These values roughly agree with those derived from the fit of the data in the case of DPPC in decane and in the case of the linoleic acid, but deeply deviate from those derived in the case of DPPA in decane.

It must be noted that in the case of a nearly full coverage of the electrode, $G_p$ approaches the values expected for water-filled pores. On the contrary, for a partial coverage, where a more complex structural arrangement of covered and uncovered regions must exist, the model suggests that the regions in absence of a well-defined lipid structure (monolayers, bilayers and multilayers) might be contacted with the electrolyte solution through a layer of solvent molecules (decane in this case) that, even if not completely, wets the metal electrode. This arrangement, whereas produces a small surface capacitance, reflects a low conductance, justifying the values of $G_p$ observed in this lipid system. Support to these pictures derives from impedance measurements of the metal electrode wetted in decane and immersed in the electrolyte solution (in absence of the lipid film deposition). By contrast, the values of $G_p$ correctly correspond to the water pore conductivity in the case of DPPC, where the residual decane is not present, owing to the high coverage value ($s = 0.99$) of the lipid film.

The presence of defects (less than 1% in the case of DPPC and close to 50% in the case of DPPA) allows a low-resistance water pathway to the ionic conduction that largely

increases the measured conductance, $G_p$, and makes it impossible to estimate the membrane conductance $G_L$.

The other parameters, $C_d$ and $G_d$, are related to the ionic layer at the lipid–electrolyte interfaces. As we have stated above, these parameters represent the equivalent circuit of the ion distribution close to the lipid–electrolyte interface after the subtraction correction performed by means of Eqs. (2)–(5). The lipid–electrolyte interface is characterized by a layer of immobilized water molecules resulting in a region with a low ionic mobility. Moreover, from a qualitative point of view, the observed relaxation times (in the range $10^{-4}$–$10^{-5}$ $s$) suggest a reduced ion mobility. This picture qualitatively justifies the values of $G_d$ (lower than that of the corresponding bulk electrolyte solution) and the observed differences between a charged (DPPA) and uncharged (DPPC) interface, even if the absolute values of the capacitance $C_d$ appear to be exceedingly small if compared with the usual double layer capacitance. Moreover, it is noteworthy that also $C_d$ values reflect the electrical properties of the lipid polar head–electrolyte interface; indeed, they are higher for charged interfaces (linoleic acid and DPPA) while they are smaller for uncharged interfaces (DPPC), corresponding to a smaller equivalent thickness of the ionic layer, in the case of charged interface.

It is noteworthy that a supported lipid membrane appears to be able to discriminate mono or divalent counterions in a bulk electrolyte solution by means of simple electrical measurements. Although bilayer lipid membrane systems have been extensively investigated as a model system of biological membranes, until recently, relative few attempts have been made to employ these structures, particularly solid-supported bilayer lipid membranes, in practical applications such as sensors and molecular devices [18]. Our work gives further support to the possibility of creating a sensor that will interact with a selected environmental counterpart, acting as a biosensor. To this end, the stability is one of the most important quality criteria since the supported membrane should remain bound to the metallic support upon storage and transfer between different media. Further improvement of the model can be obtained with self-assembled thioalkanes functionalized with specific and appropriate end groups.

## Acknowledgements

The authors are indebted to Andrea Ridi and Eric Guerci for help and experimental advice during the first measurements of this work.

## References

[1] E. Sackmann, Supported membranes: scientific and practical applications, Science 271 (1996) 43–48.
[2] C. Steinem, A. Janshoff, W.P. Sieber, M. Galla, Impedance analysis of supported lipid bilayer membranes: a scrutiny of different preparation techniques, Biochim. Biophys. Acta 1279 (1996) 169–180.
[3] L. Gu, L. Wang, A. Ottowa-Leitmannova, H.Ti. Tien, A new method for the determination of electrical properties of supported bilayer lipid membranes by cyclic voltammetry, Bioelectrochem. Bioenerg. 39 (1996) 275–289.
[4] B. Raguse, V. Braach-Maksvytis, B.A. Cornell, L.G. King, P.D.J. Osman, R.J. Pace, L. Wieczorek, Tethered lipid bilayer membranes: formation and ionic reservoir characterization, Langmuir 14 (1998) 648–659.
[5] V.J. Passechnik, T.P. Hianik, S.A. Iavanov, B. Sivak, Specific capacitance of metal supported lipid membranes, Electroanalysis 10 (1998) 295–302.
[6] B.A. Cornell, V.B.J. Braach-Maksvytis, L.G. King, P.D.J. Osman, B. Raguse, L. Wieczorek, R.J. Pace, A biosensor that uses ion-channel switches, Nature 387 (1997) 580–583.
[7] P. Krysinki, H.Ti. Tien, A. Ottowa, Charge transfer processes and redox reactions in planar lipid monolayers and bilayers, Biotechnol. Prog. 15 (1999) 974–990.
[8] R. Naumann, E.K. Schidt, A. Jonczyk, K. Fendler, B. Kadanbach, T. Liebermann, A. Offenhauser, W. Knoll, The peptide-tethered lipid membrane as a biomimetic system to incorporate cytochrome *c* oxidase in a functionally active form, Biosens. Bioelectron. 14 (1999) 651–662.
[9] J.D. Burgess, M.C. Rhoten, F.H. Hawkridge, Observation of the resting and pulsed states of cytochrome *c* oxidase in electrode-supported lipid bilayer membranes, J. Am. Chem. Soc. 18 (1998) 4488–4491.
[10] T. Hianik, M. Sneydarkova, L. Sokolikova, E. Meszar, R. Krivanek, V. Tvarozek, I. Novotny, J. Wang, Immunosensors based on supported lipid membranes, protein films and liposomes modified by antibodies, Sens. Actuators, B, Chemical 57 (1999) 201–212.
[11] L.K. Tamm, H.M. McConnell, Supported phospholipid bilayers, Biophys. J. 47 (1985) 105–113.
[12] R. Merkel, E. Sackmann, E. Evans, Molecular friction and epitactic coupling between monolayers in supported bilayers, J. Phys. (Paris) 50 (1989) 1535–1555.
[13] T.M. Bayerl, M. Bloom, Physical properties of single phospholipid bilayers adsorbed to micro glass beads. A new vesicular model system studied by 2H-nuclear magnetic resonance, Biophys. J. 58 (1990) 357–362.
[14] P. Diao, D.L. Jiang, X.L. Cui, D.P. Gu, R.T. Tong, B. Zhong, Unmodified supported thiol lipid bilayers: studies of structural disorder and conducting mechanism by cyclic voltammetry and AC impedance, Bioelectrochem. Bioenerg. 48 (1999) 469–475.
[15] S. Gritsh, P. Nollert, F. Jahnig, E. Sackmann, Impedance spectroscopy of porin and gramicidin pores reconstituted into supported lipid bilayers on indium–tin–oxide electrodes, Langmuir 14 (1998) 3118–3125.
[16] H.Ti. Tien, Z. Salamon, Self-assembling bilayer lipid membranes on solid support, Biotechnol. Appl. Biochem. 12 (1990) 478–484.
[17] H.H. Haas, G. Lamure, A. Gliozzi, Improvement of the quality of self assembled bilayer lipid membranes by using a negative potential, Bioelectrochemistry 54 (2001) 1–10.
[18] H.Ti. Tien, S.H. Wurster, A.L. Ottova, Electrochemistry of supported bilayer lipid membranes: background and techniques for biosensor development, Bioelectrochem. Bioenerg. 42 (1997) 77–94.
[19] K.L. Chiang, U.J. Krull, D.P. Nikolelis, Ellipsometric determination of the structure of surface-stabilized bilayer lipid membranes on silver metal, Anal. Chim. Acta 357 (1997) 73–77.